ELSEVIER

Ceramics International 28 (2002) 835–839

CERAMICS INTERNATIONAL

www.elsevier.com/locate/ceramint

Oxidation kinetics of MgO–C refractory bricks

Mohammad-Ali Faghihi-Sani*, Akira Yamaguchi

Department of Materials Science and Engineering, Nagoya Institute of Technology, Gokiso-Cho, Showa-ku, Nagoya 466-8555 Japan

Received 29 October 2001; received in revised form 3 November 2001; accepted 15 February 2002

Abstract

Kinetics of oxidation and disappearance of graphite in MgO–C refractory bricks have been investigated in the temperature range from 1000 to 1200 °C, where graphite is mainly consumed by gaseous oxygen in air. A mathematical model, including kinetic parameters, has been proposed to explain the extent of oxidation with time.

Keywords: Oxidation; Kinetics; Magnesia-graphite refractory brick; Oxidation rate equation; Thermo gravimeter; TG; Effective diffusivity; Convective mass transfer coefficient

1. Introduction

The combination of graphite and refractory oxides, such as MgO, provides valuable properties, such as good thermal shock resistance (resulting from the low thermal expansion and high thermal conductivity of graphite) [1] and excellent slag resistance (resulting from graphite's low wettability) [2], which are essential in steel making practice for the lining of ladles, arc furnaces and oxygen converters. Despite these advantages, graphite's susceptibility to oxidation is the major weakness of carbon-containing refractories, leading to degradation of brick properties in service. The mechanism of oxidation and disappearance of carbon in MgO–C refractories is generally classified into two categories, direct and indirect oxidation. In direct oxidation, carbon is consumed by gaseous oxygen (the so called 'gas phase oxidation'), reaction (1). While, indirect oxidation refers to reaction of carbon with solid oxygen in MgO for example (the so called 'solid phase oxidation'), reaction (2).

$$2C(s) + O_2(g) = 2CO(g) \quad \text{(Reaction 1)}$$

$$C(s) + MgO(s) = CO(g) + Mg(g) \quad \text{(Reaction 2)}$$

Fig. 1 describes the thermodynamic stability of MgO in the presence of carbon. As this figure shows, reduction of MgO [reaction (2)] becomes important at temperatures higher than 1400 °C and reaction (1) is the major mechanism of oxidation at temperatures lower than 1400 °C.

Although both mechanisms are important, direct oxidation is widely used for comparison of oxidation resistance of these refractories. Many studies have been presented concerning the effects of: partial pressure and accessibility of oxygen to graphite flake edges [3]; open porosity, shape and orientation of the products [4]; flow characteristics of the gaseous species around the products [5] and reactivity of the flakes [6] on the direct oxidation rate. However, only a few studies have attempted to describe the kinetic process by presenting a model and deriving equations [3], [5], [7]. Among them, Li et al. [5] have proposed the most comprehensive model, although their experimental apparatus was very complicated. In the present work, the authors have tried to propose a mathematical model for the direct oxidation kinetics of magnesia-graphite refractories by establishing a simple and practical laboratory apparatus.

2. Experimental procedure

2.1. Sample preparation

Experimental bricks were prepared using the raw materials listed in Table 1. Cylindrical samples, 20 mm in diameter and 20 mm in height, were prepared by drilling parallel to the brick's pressing axis. The prepared samples were heated at 400 °C for 3 h in CO gas to remove

* Corresponding author. Tel.: +81-052-735-5280; fax: +81-052-735-5294.

E-mail address: ramin_sani@hotmail.com (M.-A. Faghihi-Sani).

0272-8842/02/$22.00
PII: S0272-8842(02)00049-4

volatile species resulting from the binder. Finally, the samples were heated for 3 h at 1300 °C to stabilize their structures. Before the oxidation test, open pore size distributions of these samples were determined by mercury porosimetry.

2.2. Oxidation test apparatus

Fig. 2 describes the experimental apparatus of the isothermal oxidation test. To remove the anisotropy of oxidation resistance due to the preferred orientation of graphite flakes in the brick, the circular ends of the cylindrical samples were covered by alumina plates and only the straight sides (which were parallel to the pressing axis) were exposed to the airflow during oxidation. The furnace was preheated to the desired temperatures (1000, 1100 and 1200 °C) and then raised around the sample. The mass changes during oxidation at each temperature were automatically recorded every 1 min. Also, a series of samples were oxidised at 1000 °C for 2, 4, 6, 8 and 10 h, and the radius of unoxidized area after each oxidising period was directly measured.

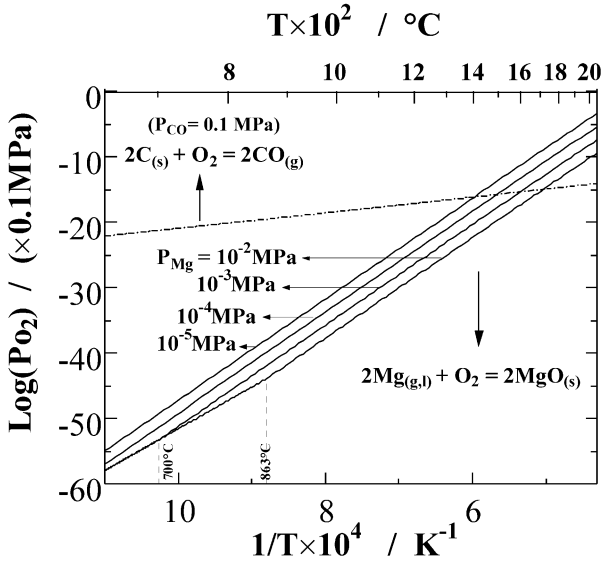

Fig. 1. Thermodynamic stability of MgO in presence of C under various P_{Mg}.

Table 1
Composition of the MgO–C refractory bricks

Raw materials	Particle size	Purity (%)	Wt.%
MgO			
Fused MgO	1–2 mn	>99	60
Sintered MgO	<65 μm	>99	20
C			
Graphite	180–300 μm	>99	10
Graphite	<180 μm	>99	10
Binder			
Phenolic resin	Liquid	–	4

3. Kinetic modelling of the oxidation process

Fig. 2(b) shows the cylindrical sample at time t of oxidation process, where r_0 and l are the radius and length of the sample and r_t is the radius of unoxidized area. Since inward advancement of the reaction interface is slow and continuous, the oxidation process can be considered as steady state for a short period of time (dt) around t. The following five steps of the oxidation process may proceed at the same rate:

(I) Inward mass transport of O_2 from the bulk airflow to the sample's surface:

$$q_1^{(O_2)} = 2\pi \cdot r_0 \cdot l \cdot k_m \cdot \left[C_b^{(O_2)} - C_s^{(O_2)} \right] \quad (1)$$

where $q_1^{(O_2)}$is the molar amount of O_2 that reaches the sample's surface (S_0) within unit of time around t.

(II) Inward diffusion of O_2 through the porous oxidized layer from the sample's surface (S_0) to the reaction interface (S_t):

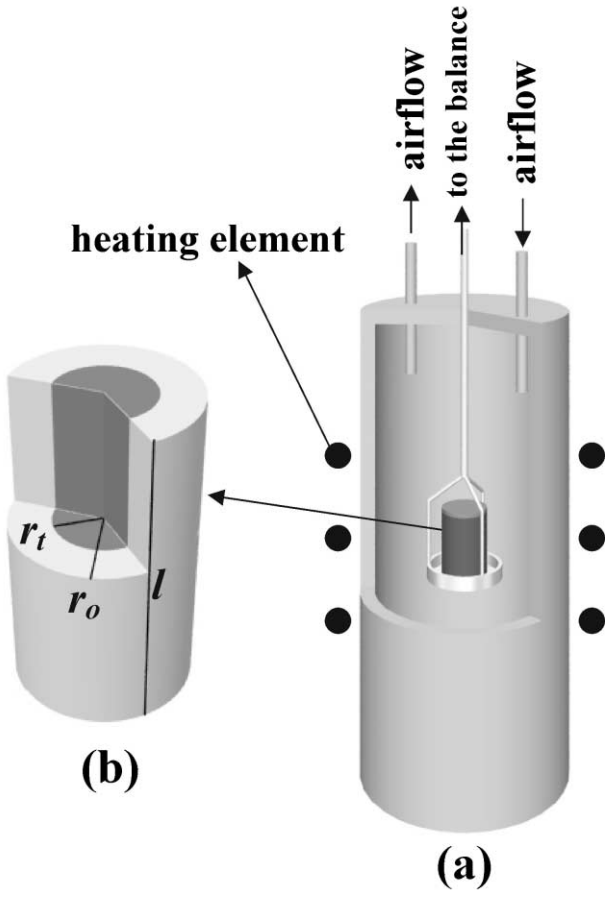

Fig. 2. (a) Schematic of the experimental apparatus, used for the isothermal oxidation test; (b) model of the oxidized sample at the time t of oxidation process.

$$q_2^{(O_2)} = \frac{2\pi \cdot l \cdot D \cdot \left[C_S^{(O_2)} - C_t^{(O_2)}\right]}{\ln\left(\frac{r_0}{r_t}\right)} \quad (2)$$

where $q_2^{(O_2)}$ is the molar amount of O_2 that reaches the reaction interface (S_t) within unit of time around t.

(III) Chemical reaction between graphite and O_2 [reaction (1)] at the reaction interface (S_t):

$$q_R^{(O_2)} = 2\pi \cdot r_t \cdot l \cdot k_c \cdot \left[C_t^{(O_2)} - \frac{1}{k_E} \cdot C_t^{(CO)}\right] \quad (3)$$

where $q_R^{(O_2)}$ is the molar amount of O_2 that reacts with C at the reaction interface (S_t) within unit of time around t.

(IV) Outward diffusion of CO through the porous oxidized layer from the reaction interface (S_t) to the sample's surface (S_0):

$$q_1^{(CO)} = \frac{2\pi \cdot l \cdot D \cdot \left[C_t^{(CO)} - C_s^{(CO)}\right]}{\ln\left(\frac{r_0}{r_t}\right)} \quad (4)$$

where $q_1^{(CO)}$ is the molar amount of CO that reaches the sample's surface (S_0) within unit of time around t.

(V) Outward mass transport of CO from the sample's surface (S_0) into the surrounding atmosphere:

$$q_2^{(CO)} = 2\pi \cdot r_0 \cdot l \cdot k_m \cdot \left[C_s^{(CO)} - C_b^{(CO)}\right] \quad (5)$$

where $q_2^{(CO)}$ is the molar amount of CO that transfers from the sample's surface (S_0) to the surrounding atmosphere within unit of time around t.

In the previous five equations, C_b, C_s and C_t represent the O_2 or CO molar concentration inside the air flow, at the sample's surface, and at the reaction interface, respectively, at time t of the oxidation process. Constants k_m, D, k_c and k_E are the convective mass transfer coefficient, effective diffusivity, rate constant of chemical reaction and equilibrium constant of reaction (1), respectively.

Considering the earlier five steps, taking reaction (1) into account, and based on the mass balance of materials we have:

$$2q_1^{(O_2)} = 2q_2^{(O_2)} = 2q_R^{(O_2)} = q_1^{(CO)} = q_2^{(CO)} \quad (6)$$

Combining Eqs. (1)–(6) and considering that reaction (1) is irreversible and consequently k_E is very large, it can be concluded that:

$$q_R^{(O_2)} = \frac{2\pi \cdot l \cdot C_b^{(O_2)}}{\frac{\ln(r_0/r_t)}{D} + \frac{1}{r_0 \cdot k_m} + \frac{1}{r_t \cdot k_c}}$$

$$q_R^{(C)} = 2q_R^{(O_2)}$$

$$R_t^{(C)} = \frac{1}{S_t} \times q_R^{(C)} = \frac{1}{2\pi \cdot r_t \cdot l} \times q_R^{(C)}$$

$$\Rightarrow R_t^{(C)} = \frac{2C_b^{(O_2)}}{\frac{r_t \cdot \ln(r_0/r_t)}{D} + \frac{r_t}{r_0 \cdot k_m} + \frac{1}{k_c}} \quad (7)$$

where $q_R^{(C)}$ is the molar amount of C that reacts with oxygen at the reaction interface (S_t) within unit of time around t. The rate of oxidation [$R_t^{(C)}$] may also be equated to the rate of disappearance of solid carbon (in mole) per unit of time per unit of surface area:

$$R_t^{(C)} = \frac{1}{S_t} \times \frac{-dn_t}{dt} \ \& \ dn_t = \rho_M \times S_t \times r_t$$

$$\Rightarrow R_t^{(C)} = -\rho_M \times \frac{dr_t}{dt} \quad (8)$$

where ρ_M is the molar density of graphite in the MgO–C refractory brick.

By combining Eqs. 7 and 8 we have:

$$\int_0^t \frac{2C_b^{(O_2)}}{\rho_M} \times dt$$

$$= -\int_{r_0}^{r_t} \left(\left(\frac{\ln r_0}{D} + \frac{1}{r_0 \cdot k_m}\right) \times r_t - \frac{1}{D} \times r_t \cdot \ln r_t + \frac{1}{k_c}\right) \cdot dr_t \Rightarrow$$

$$\frac{2C_b^{(O_2)}}{\rho_M} \cdot t = \frac{1}{2D} \cdot r_t^2 \cdot \ln r_t - \left(\frac{\ln r_0}{2D} + \frac{1}{2r_0 \cdot k_m} + \frac{1}{4D}\right) \cdot r_t^2$$

$$- \frac{1}{k_c} \cdot r_t + \left(\frac{r_0}{2k_m} + \frac{r_0^2}{4D} + \frac{r_0}{k_c}\right) \quad (9)$$

The Eq. 9 presents a mathematical relation between the radius of unoxidized area (r_t) and oxidation time (t), including physical ($C_b^{(O_2)}$, ρ_M) and kinetic (k_m, D, k_c) parameters. The effective diffusivity (D) reflects the structural aspects of the MgO–C refractory samples, which is related to the volume of open porosity as well as the shape and orientation of open pores in the oxidized layer. On the other hand the rate constant of chemical reaction (k_c) represents the chemical aspects of the refractory sample such as reactivity and impurity of the graphite. The convective mass transfer coefficient (k_m) reflects the environmental conditions such as viscosity, density and flow rate of the oxidizing gas and the sample dimension.

4. Results and discussion

The open porosity and pore size distribution of the prepared samples for oxidation test is presented in Fig. 3.

Fig. 4 shows experimental results of the isothermal oxidation process in air at various temperatures. Although the results present the mass changes (ΔW_t) as a function of oxidation time (t), a numerical relation between radius of unoxidized area (r_t) and t can also be derived from the results, considering the proposed model in Fig. 2(b) and following equations at the oxidation time of t:

Volume fraction of unoxidized graphite

$$= \frac{\text{volume of unoxidized area}}{\text{total volume of sample}} = \frac{\pi \cdot r_t^2 \cdot l_0}{\pi \cdot r_0^2 \cdot l_0} = \frac{r_t^2}{r_0^2}$$

Mass fraction of unoxidized graphite

$$= \frac{\text{mass of unoxidized graphite}}{\text{initial mass of graphite}} = \frac{m \cdot W_0 + \Delta W_t}{m \cdot W_0}$$

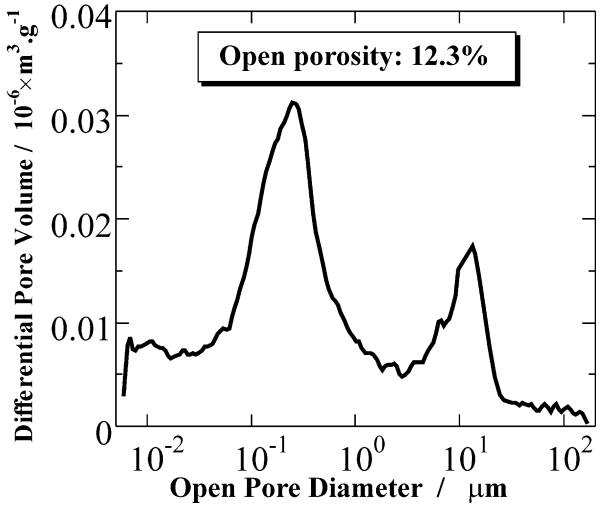

Fig. 3. Open pore size distribution of MgO–C samples prepared for oxidation test.

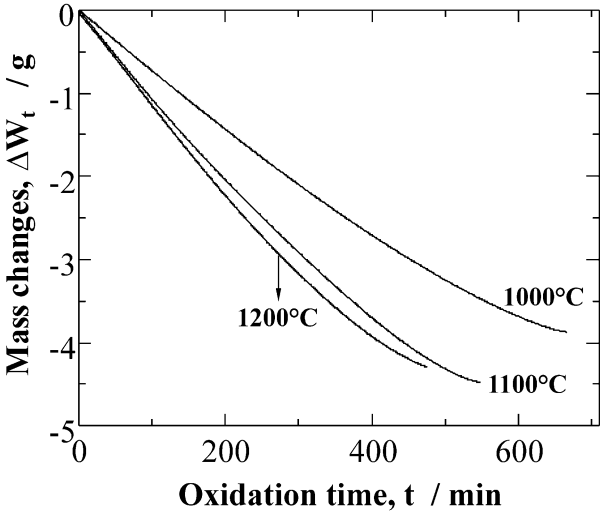

Fig. 4. Mass changes of the prepared MgO–C refractory samples during isothermal oxidation in air at various temperatures.

where m is the initial mass fraction of graphite in the sample; W_0 is the initial mass of sample; and ΔW_t is the amount of mass change (graphite burnout) by time t.

Since left sides of the above equations are equal we have:

$$\frac{r_t^2}{r_0^2} = \frac{m \cdot W_0 + \Delta W_t}{m \cdot W_0} \Rightarrow$$

$$r_t = r_0 \times \left(\frac{m \cdot W_0 + \Delta W_t}{m \cdot W_0} \right)^{1/2} \tag{10}$$

Considering Eq. 10 and the experimental results in Fig. 4, the oxidation time (t) versus the radius of unoxidized area (r_t) at various temperatures can be plotted as in Fig. 5. Direct measurement of the radius of unoxidized area after various oxidation periods (2, 4, 6, 8 and 10 h) at 1000 °C are also presented in Fig. 5, confirming the validity of the earlier modelling.

The relationship between t and r_t in Fig. 5 is expected to follow the typical form of Eq. 9, as presented in Eq. 11.

$$t = a \cdot r_t^2 \cdot \ln r_t + b \cdot r_t^2 + c \cdot r_t + d \tag{11}$$

Adopting a non-linear regression method, based on Eq. 11, on the calculated data in Fig. 5 indicates parameters a, b, c and d, and consequently the kinetic parameters mentioned in Eq. 9. As shown in Fig. 5, the fitting curves are in good agreement with the data. The calculated parameters a, b, c and d at various temperatures are listed in Table 2.

$C_b^{(O_2)}$at the experimental temperatures can be determined as: $C_b^{(O_2)} = \frac{n}{V} = \frac{P(O_2)}{RT}$ where R is the gas constant and $P(O_2)$ is the partial pressure of oxygen in the airflow (0.21×10^5 Pa). The carbon molar density (ρ_M) of the

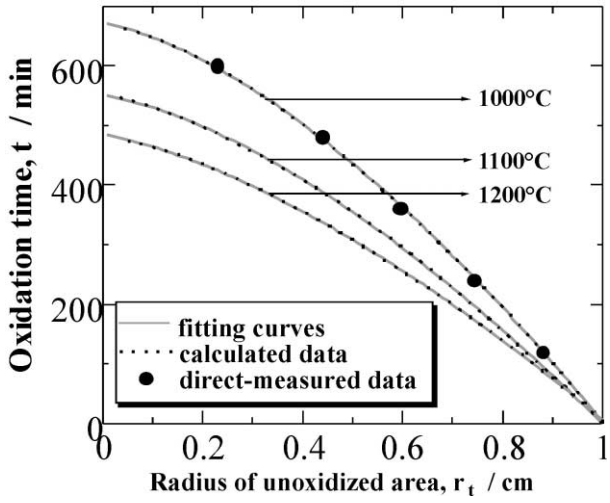

Fig. 5. Variation of oxidation time with radius of unoxidized area. Calculated data are based on the data of Fig. 4 and Eq. 10.

Table 2
Calculated values of parameters in Eq. 11 and kinetic parameters at various temperatures

Temperature (°C)	a (min cm^{-2})	b (min cm^{-2})	c (min cm^{-1})	d (min)	D (cm^2 min^{-1})	k_m (cm min^{-1})
1000	161.42	−505.71	−165.78	673.36	35.12	13.34
1100	138.28	−412.62	−140.20	551.74	46.19	18.60
1200	98.04	−317.75	−163.45	486.33	66.47	24.25

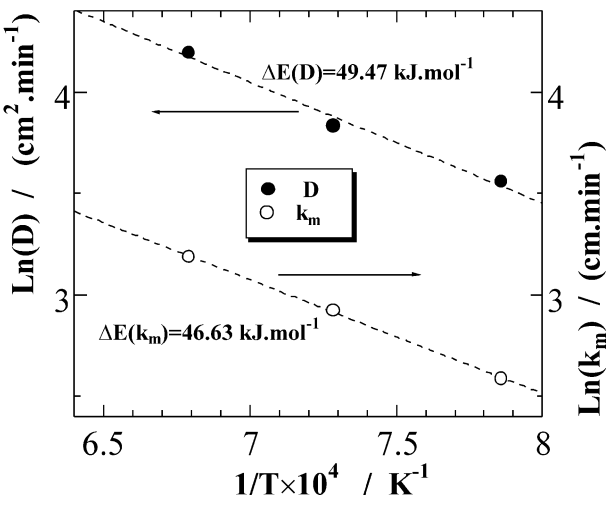

Fig. 6. Arrhenius plots of the effective diffusivity (D) and the convective mass transfer coefficient (k_m).

experimental samples in this study was 0.0470 mole·cm^{-3}. Considering the earlier calculated parameters, D and k_m at various temperatures can be determined (Table 2). Since the rate of reaction (1) is high at the experimental temperatures and, consequently, it does not control the overall oxidation process, the rate constant of chemical reaction (k_m) has not been determined. The obtained D and k_m values in this study are, respectively, twice and half of the results reported by Li et al. [5]. The obtained kinetic parameters D and k_m are expected to show an Arrhenius type relation with temperature. Fig. 6 presents this temperature dependence of the kinetic parameters. As a result, the value of activation energy for D and k_m can be calculated by adopting a linear regression on the data in Fig. 6. As shown in this figure, D and k_m follow perfectly the Arrhenius-type relation with temperature. The obtained activation energy for D is similar to the value reported by Li et al. [5].

5. Conclusions

This study has attempted to model the kinetic aspects of direct oxidation of MgO–C refractory bricks. In this regard, five steps have been defined to express the oxidation process. Each step has been equated according to the proposed model. Further, an equation including kinetic parameters has been derived to explain the extent of oxidation with time. The experimental results of isothermal oxidation of MgO–C refractory samples at various temperatures have been rationalized using the derived equation. As a result, the kinetic parameters, D andK_m, have been determined at various temperatures. Regarding the Arrhenius type relation of the D andK_m with temperature, the activation energy of them has also been determined as 49.47 and 46.63 k J·mol^{-1}, respectively.

References

[1] C.F. Cooper, I.C. Alexander, C.J. Hampson, The role of graphite in the thermal shock resistance of refractories, Br. Ceram. Trans. J. 84 (2) (1985) 57–62.
[2] B. De Benedetti, G. Acquarone Burlando, Corrosion resistance of resin-bonded magnesia–carbon refractories, Br. Ceram. Trans. J. 88 (1989) 55–57.
[3] K. Ichikawa, H. Nishio, Y. Hoshiyama, Oxidation test of MgO–C bricks, Taikabutsu Overseas 14 (1) (1994) 13–19.
[4] X. Li, M. Rigaud, Anisotropy of the properties of magnesia–graphite refractories: linear thermal change and carbon oxidation resistance, J. Can. Ceram. Soc. 62 (3) (1993) 197–205.
[5] X. Li, M. Rigaud, S. Palco, Oxidation kinetics of graphite phase in magnesia–carbon refractories, J. Am. Ceram. Soc. 78 (4) (1995) 965–971.
[6] X. Li, M. Rigaud, Effect of graphite quality on oxidation and corrosion resistance of magnesia–carbon refractories, in: M. Rigaud, C. Allaire (Eds.), Proceedings of the Second International Symposium on Advances in Refractories for the Metallurgical Industries, Canada, Ecole Polytechnique, Montreal, Quebec, Canada, 1996, pp. 95–107.
[7] O.S. Özgen, B. Rand, Kinetics of oxidation of the graphite phase in alumina/graphite materials, I—effect of temperature and initial pore structure at a fixed graphite content, Br. Ceram. Trans. J. 84 (2) (1985) 70–76.